On the influence of high-pass filtering on ICA-based artifact reduction in EEG-ERP

Irene Winkler, Stefan Debener, Klaus-Robert Müller, and Michael Tangermann

***Abstract*— Standard artifact removal methods for electroencephalographic (EEG) signals are either based on Independent Component Analysis (ICA) or they regress out ocular activity measured at electrooculogram (EOG) channels. Successful ICA-based artifact reduction relies on suitable pre-processing. Here we systematically evaluate the effects of high-pass filtering at different frequencies. Offline analyses were based on event-related potential data from 21 participants performing a standard auditory oddball task and an automatic artifactual component classifier method (MARA). As a pre-processing step for ICA, high-pass filtering between 1-2 Hz consistently produced good results in terms of signal-to-noise ratio (SNR), single-trial classification accuracy and the percentage of 'near-dipolar' ICA components. Relative to no artifact reduction, ICA-based artifact removal significantly improved SNR and classification accuracy. This was not the case for a regression-based approach to remove EOG artifacts.**

I. INTRODUCTION

Electroencephalography (EEG) measurements of brain activity are contaminated by undesired additional signals. These artifacts are caused by non-neural physiological activities of the subject, such as movements of the eyes and muscles, heart beat and pulse, and by external technical sources.

A common approach for artifact reduction is the transformation of EEG signals into a space of independent source components (ICs) using Independent Component Analysis (ICA). Ideally ICA separates artifactual and neural activity into distinct ICs, so that artifactual ICs can be identified [1] and a cleaner EEG can be constructed without them. In practice, ICs are often mixtures of both neural and artifactual sources. However, pre-processing of EEG data prior to ICA can improve the quality of the artifact separation [2], e.g. by removal of obvious, high-amplitude artifactual epochs, or by dimensionality reduction with Principal Component Analysis (PCA). Here we focus on the role of high-pass filtering.

Without prior high-pass filtering, ICA often produces visibly poor separation, with many mixed components, such as the ones displayed in the right part of Fig. 2. Recent research indicates that high-pass filtering improves reliability [3] and measures of independence and dipolarity [4] of the estimated independent components. Furthermore, trial-by-trial fluctuations of the blood-oxygen-level dependent (BOLD) signal were found to be positively correlated with high EEG gamma power when ICA de-mixing was obtained on gamma band-pass filtered EEG data, but not when 30 Hz low-pass filtered data was fed into ICA [5]. In this paper, we systematically analyze the effect of ICA-based artifact reduction on Event-Related Potentials (ERPs), as well as the percentage of 'near-dipolar' ICA-components [6], as a function of the high-pass filter frequency.

Our focus is not on how to obtain best classification performance. Instead, we will use single-trial classification performance as a proxy for successful artifact reduction. In addition, we focus on the signal-to-noise ratio (SNR) of ERPs. For varying cutoff frequencies, we train ICA on high-pass filtered data, automatically classify the resulting ICs with MARA [7], [8], and apply the obtained filter weights on the original non high-pass filtered data (see Fig. 1).

Similar to an analysis presented in [9], we also compare ICA-based artifact removal with a regression-based method, which uses electrooculogram (EOG) signals to partially remove ocular activity [10].

II. METHODS

A. *Why high-pass filtering influences ICA decomposition*

Given EEG signals $x_1, \ldots, x_K$ recorded from K electrodes over time, ICA methods linearly decompose the data into K source components $s_1, \ldots, s_K$. To solve this blind source separation problem, ICA assumes the mutual independence of source components and a linear generative model $x_j = \sum_{k=1}^{K} \mathbf{a}_k[j] \cdot s_k \quad (j \in \{1, \ldots, K\})$. Here $\mathbf{a}_k \in \mathbb{R}^K$ denotes the spatial activation pattern of source k and $\mathbf{a}_k[j]$ its jth element.

High-pass filtering is a linear transformation of the signals. Therefore, if the assumed generative model was true, filtering

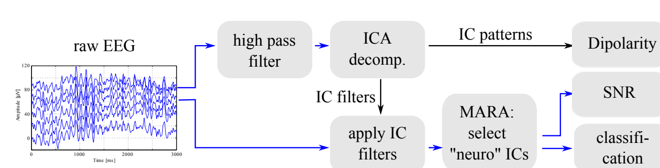

Fig. 1: Schematic workflow for high-pass filtering of EEG data prior to ICA decomposition. IC filters are applied on the unfiltered raw data before their classification by MARA.

This work was supported by the Brain Korea 21 Plus Program through the National Research Foundation of Korea funded by the Ministry of Education and by the German Research Council (DFG) within the Cluster of Excellence BrainLinks-BrainTools (EXC 1086).

Irene Winkler (irene.winkler@tu-berlin.de) and Klaus-Robert Müller (klaus-robert.mueller@tu-berlin.de) are with the Machine Learning Group, Berlin Institute of Technology, Germany. Klaus-Robert Müller is also with the Department of Brain and Cognitive Engineering, Korea University, Republic of Korea. Stefan Debener (stefan.debener@uni-oldenburg.de) is with the Cluster of Excellence Hearing4all, University of Oldenburg and the Neurophysiology Lab, Department of Psychology, European Medical School, University of Oldenburg, Germany. Michael Tangermann (michael.tangermann@blbt.uni-freiburg.de) is with the Brain State Decoding Lab, BrainLinks-BrainTools Cluster of Excellence and Computer Science Dept., University of Freiburg, Germany.

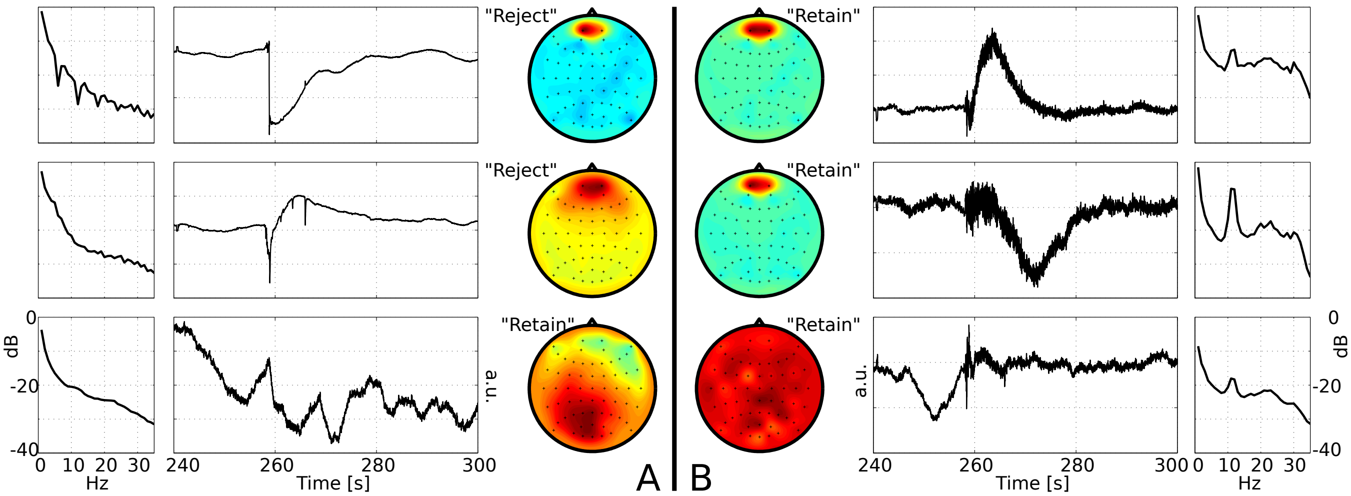

Fig. 2: Example for ICA decompositions of one study participant gained (A) with vs. (B) without 1 Hz high-pass preprocessing. Scalp patterns, spectrum and time course of the three components explaining most variance are shown together with labels (reject vs. retain) estimated by MARA, which labels components conservatively: mixed components, which contain both artifactual and neuronal activity tend to be retained in the data. In contrast to ICA after high-pass filtering, ICA on the unfiltered data did not separate oscillatory activity from the electrode pop artifact.

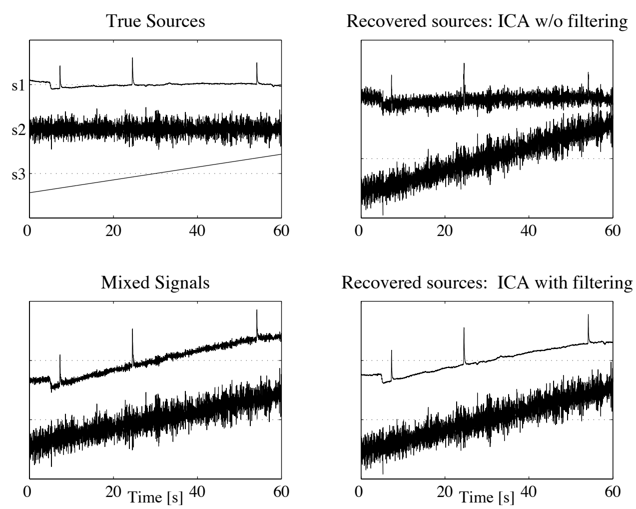

Fig. 3: Toy example of an underdetermined ICA problem with two sensors but three independent sources: (s1) eye blinks, (s2) oscillatory neural activity, and (s3) a linear drift. ICA without prior high-pass filtering separates the drift from the eye blink component, but both components contain neural activity. In contrast, ICA applied after 1 Hz high pass filtering separates the eye blink from the neural component.

would not change the ICA model coefficients: Under the model assumptions, it also holds for the filtered signals $h(x_j)$ that $h(x_j) = h\left(\sum_{k=1}^{K} \mathbf{a}_k[j] \cdot s_k\right) = \sum_{k=1}^{K} \mathbf{a}_k[j] \cdot h(s_k)$, where $h(\cdot)$ denotes linear filtering. The filtered source signals $h(s_k)$ remain mutually independent, and the coefficients of the mixing matrix $\mathbf{a}_k[j]$ are unchanged. It is therefore valid to use the filtered data for the estimation of ICA only, and then apply the obtained demixing matrix to the unfiltered data (see [2], [11] for more information).

In practice, high-pass filtering does make an important difference. It is, however, not entirely understood why this is the case. High-pass filtering can help ICA estimation by increasing the independence between sources, because slowly changing trends are not very independent [2], [11]. Furthermore, standard ICA assumptions such as the limited number of sources are at best approximately met in practice. Filtering 'guides' the ICA decomposition towards extracting the components that explain the activity we are interested in and may help to better satisfy ICA's stationarity assumption. The low-frequency parts of an EEG signal contain a large portion of its variance, that we are typically not so interested in. It is thus often beneficial to remove them. A simple toy example, which illustrates this point, is presented in Fig. 3.

B. Data

Data of 21 healthy subjects were recorded during a standard auditory oddball paradigm as part of an auditory Brain Computer Interface (BCI) study [12]. The experiment was conducted according to the Declaration of Helsinki, participants provided their written informed consent prior to participation. They were asked to avoid blinking while attending rare high-frequent target tones and disregard frequent non-target tones. This measurement lasted approx. 10 minutes. Per participant, 400 non-target and 100 target stimuli were presented in randomized order at a Stimulus Onset Asychnrony (SOA) of 1 s. It can be expected, that attended target tones lead to a more negative ERP component around 100 ms post stimulus (N1) compared to non-target responses, and to a positive ERP component (P3) at approx. 300 ms post stimulus. EEG was recorded with nose reference from 61 scalp channels and one electrode below the right eye (EOGvu). Signals were downsampled to 100 Hz and low-pass filtered at 45 Hz (forward-backward two-pass 5th order Butterworth filter) for all variants of the following offline analysis. As no rejection of any epoch or channel was performed, artifacts remained in the data.

C. Evaluation metrics

Visual inspection: The tested artifact removal variants were independently applied to the continuous data. For plotting grand average ERP responses and further ERP processing, data was epoched around the stimulus, and baseline activity was removed according to an interval of 150 ms duration pre-stimulus.

SNR: Suitable artifact processing has the potential to decrease single-trial noise around the average ERP response. For each artifact removal variant, we assessed this effect by computing the signal-to-noise ratio (SNR). We measure SNR as proposed by [13]: Given N epochs, $y_1, \ldots, y_N \in \mathbb{R}^T$, each measured over T time points at one channel, the SNR is given as

$$\text{SNR} = \frac{\text{Var}_t\{\bar{y}(t)\}}{\frac{1}{N}\sum_{n=1}^{N} \text{Var}_t\{y_n(t) - \bar{y}(t)\}} \tag{1}$$

where $\bar{y}(t) = \frac{1}{N}\sum_{n=1}^{N} y_n(t)$ is the ERP averaged over epochs at time t. This defines the ratio of the variance of the ERP (*signal*) and the mean variance of residual deviation (*noise*).

We report SNR values for the N1–P2 complex at channel FC3 in the interval [100–250 ms], and separately for target and non-target epochs. We use the target class to compute SNR for P3 at channel Cz in the interval [250–550 ms].

Classification: The accuracy for the binary target vs. non-target classification task was estimated by chronological 10-fold cross-validation of a linear classifier (shrinkage regularized Linear Discriminant Analysis) trained on features which consist of windowed means derived from specific non-overlapping consecutive intervals [14]. Classification was performed in three conditions, which used different ERP feature intervals (all values in ms): (1) the N1-P2 complex (100–130, 140–170, 180–210, 220–250 $\Rightarrow 4 \cdot 61 = 244$ features), (2) the P3 component (260–340, 350–430, 440–550 $\Rightarrow 3 \cdot 61 = 183$ features) and (3) combined ($\Rightarrow 7 \cdot 61 = 427$ features). Accuracy is defined as the percentage of correctly classified epochs and is reported class-wise normalized, i.e. the accuracies were calculated for both classes separately and the results were averaged.

Dipolarity: We also compare ICA decompositions with a measure that does not depend on the classification of artifactual components or subsequent EEG analysis: the percentage of 'near-dipolar' components as proposed by [6]. It is defined as the percentage of components whose scalp patterns can be explained by a single equivalent dipole (which we identify with MUSIC [15]) with less than a specified error variance (which we set to 20%). As discussed in [6] in detail, this 'dipolarity' of the ICA decomposition is a very informative, albeit simplistic measure of physiological plausibility.

D. ICA and the effect of high-pass filtering

To evaluate the effect of high-pass filtering, we computed the ICA demixing on high-pass filtered data at 37 different cutoff frequencies (0.1, 0.2, . . ., 2, 2.5, . . ., 6, 7, . . ., 10, 15, . . ., 40 Hz). Filtering was carried out with a second order Butterworth filter. We chose FastICA [16] as it is frequently used ICA method for the analysis of EEG data.

The obtained de-mixing coefficients were then applied to the *unfiltered* data, as proposed e.g. in [17] and illustrated in Fig. 1. In this way, we only consider the effect of filtering on the ICA decomposition. (Note that de-mixing coefficients are often applied to the filtered data, in which case filtering affects all subsequent analysis. Filtering may distort the shape of ERP components, including peak amplitudes and onset latencies [18], but can improve classification performance [19], [20]. This is not the focus of our attention here.)

The resulting source components were labeled with MARA [7], [8]. MARA is a heuristic, that solves the binary classification problem 'reject vs. accept' fast and objectively. It is able to handle eye artifacts, muscular artifacts and loose electrodes. When confronted with mixed components, MARA decides conservatively and retains them in the data, as shown in Fig. 2. Subsequently, (cleaner) EEG data was reconstructed by omitting components labeled as artifacts.

E. Comparison with regression

We compare ICA-/MARA-based artifact cleaning (with 1 Hz and 2 Hz pre-filtering) to a regression approach for the removal of eye activity measured at additional electrooculogram (EOG) channels [10]. A standard procedure is to subtract part of the vertical (VEOG) and horizontal EOG (HEOG) from each recorded EEG electrode x_j as

$$z_j(t) = x_j(t) - \hat{\alpha}_j VEOG(t) - \hat{\beta}_j HEOG(t) - \hat{\gamma}_j \tag{2}$$

where z_j denotes the 'cleaned' EEG signal at electrode j, and $\hat{\alpha}_j, \hat{\beta}_j$ and $\hat{\gamma}_j$ are regression coefficients estimated by ordinary least squares.

Regression-based methods are limited by the fact that EOG is contaminated by brain activity which is removed as well. To alleviate bidirectional contamination, EOG channels are typically low-pass filtered prior to the regression step. Motivated by [9], [21], we used a cut-off at 7.5 Hz.

For this analysis EOG was derived as a post-hoc bipolar derivation from channels (F9, F10) for horizontal EOG and (Fp2, EOGvu) for vertical EOG. Channels F9, F10 and Fp2 were excluded from the set of EEG channels.

III. RESULTS

A. ICA and the effect of high-pass filtering

Grand-average ERPs for several artifact removal variants are depicted in Fig. 5. The influence of high-pass filtering on the ICA decomposition is not strongly reflected in the shape of ERPs. Peak amplitudes were only slightly attenuated even when ICA was trained on 30 Hz high-pass filtered data. Similarly, strong drifting components were removed both when ICA was trained on filtered and unfiltered data.

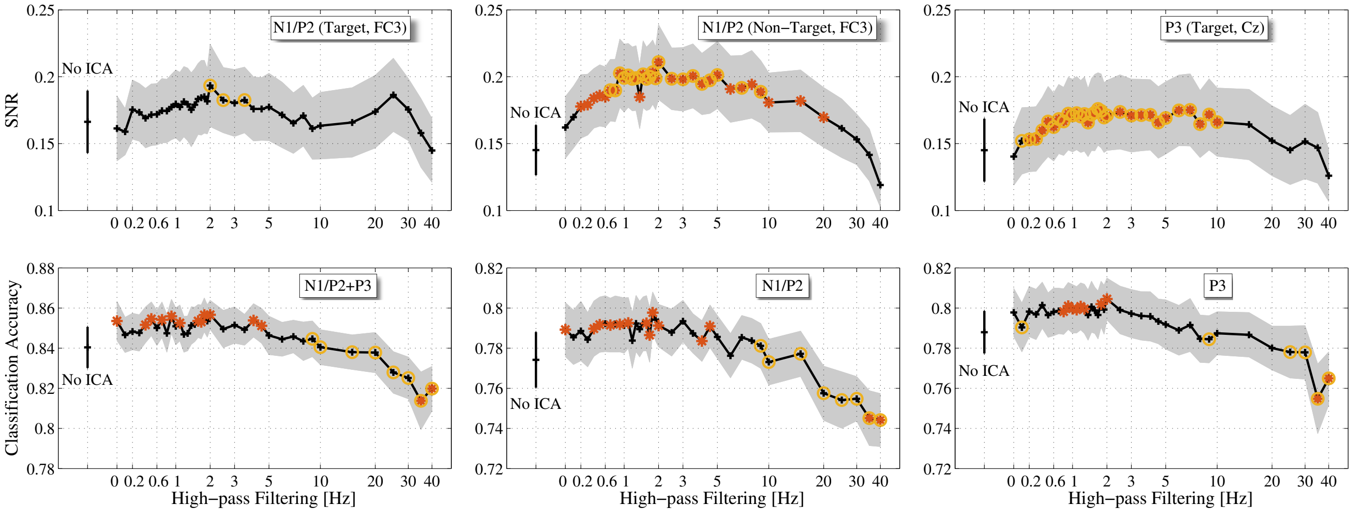

Fig. 4: SNR values (top row) and performance of target vs. non-target classification (bottom row) including means and $\pm$ standard errors (s.e.) as a function of high-pass filtering cut-off frequency applied before ICA. Condition '*0*' refers to no high-pass filtering before ICA artifact removal, and condition '*No ICA*' omits the ICA artifact removal completely. A red star indicates values which significantly differ from condition '*No ICA*', a yellow circle indicates values which differ from condition '*0*', according to a Wilcoxon signed rank test at $p < 0.05$. No multiple-testing corrections were applied.

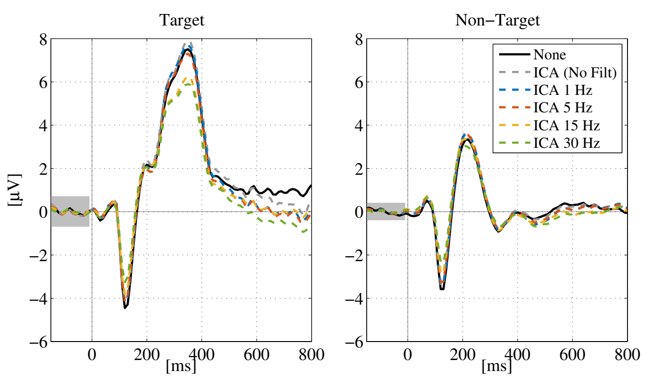

Fig. 5: Target- and non-target grand average (n=21) ERP responses at channel Cz from either raw data or after ICA-based cleaning. ICA weights were always applied to the unfiltered data, however ICA was trained on high-pass filtered data at different cutoff frequencies.

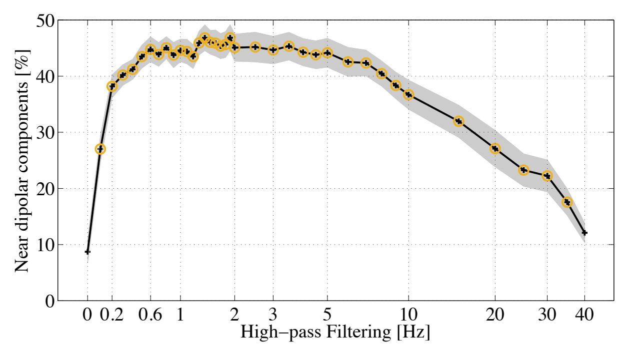

Fig. 6: Percentage of components whose scalp patterns can be explained from the scalp projection of one equivalent dipole with less than 20% error variance ($\pm$ s.e.), as a function of high-pass filtering frequency applied before ICA. A yellow circle indicates values which significantly differ from condition '*0*' (no high-pass filtering), as in Fig. 4.

Obtained SNR values, classification performances and percentages of near-dipolar components are depicted in Fig. 4 and Fig. 6. Values on the x-axis indicate the type of high-pass filtering applied. For N1-P2 SNR (non-targets), P3 SNR (targets) and the percentage of near-dipolar components we see a consistent increase for small frequencies. The effect is particularly strong (and highly significant) for the percentage of near-bipolar ICA components, which ranges from 9% without to 47% with 1.9 Hz pre-filtering. Similarly, best SNR values are achieved between 1 and 5 Hz. ICA artifact removal applied to high-pass filtered data in these ranges significantly improves SNR as compared to no artifact reduction and compared to ICA without high-pass filtering.

We observe no strong differences between early and late ERP components. However, SNR values of the N1-P2 complex of the target class are less sensitive than for the non-target class. This may be because there are four times as many epochs in the non-target class, which allows for a more accurate SNR estimate. Classification accuracy is also not very sensitive to the artifact reduction variants we analyzed. Nevertheless, ICA artifact removal significantly improved over no artifact reduction mostly when applied to high-pass filtered data in frequencies between 0.5 and 2 Hz.

B. Comparison with regression

A comparison of ICA-based (with 1 Hz and 2 Hz pre-filtering) with regression-based artifact removal in terms of SNR and classification performance is summarized in Table I. ICA with 2 Hz pre-filtering yielded higher SNR and classification accuracy than 1 Hz pre-filtering, however this

TABLE I: SNR and overall classification accuracy (mean ± s.e.) for different artifact reduction methods. $<, >$ indicate significant differences ($p < 0.05$, Wilcoxon signed rank).

	None (N)	ICA (I1) -1 Hz-	ICA (I2) -2 Hz-	Regr. (R)
Accuracy	84.2±1.0	85.3±0.9	**85.7**±0.7	84.7±1.0
(in %)	< I1 I2	> N	> N	
SNR N1/P2	0.17±0.02	0.17±0.03	**0.19**±0.03	0.16±0.02
(Target)		< I2	> I1 R	< I2
SNR N1/P2	0.15±0.02	0.19±0.02	**0.21**±0.03	0.15±0.02
(Non-Target)	< I1 I2	>N R , < I2	> N I1 R	< I1 I2
SNR P3	0.15±0.02	0.17±0.03	**0.17**±0.03	0.15±0.02
(Target)	< I1, I2	> N	> N R	< I2

effect is not consistently significant. Classification accuracy increased after ICA for both pre-filtering variants, which was not the case for the regression-based approach. In terms of SNR, ICA with 2 Hz pre-filtering significantly improved over regression-based artifact removal.

IV. DISCUSSION

In this paper, we have quantified the impact of high-pass filtering on artifact reduction, focussing on ERPs obtained from a standard auditory oddball task resulting in typical target and non-target event-related responses. With adequate pre-filtering, artifact cleaning based on ICA and MARA improved both, classification accuracy and signal-to-noise ratio (SNR). Consistent with [9], this was not the case for the regression-based method we analyzed in addition.

In general, SNR was more sensitive to variations in artifact removal than classification accuracy or the shape of the ERP. As the obtained high classification rates are not strongly influenced by cleaner data, we conjecture that a relative large distance between class means dominates the investigated classification problem. Of course, this situation may be different with other ERP data sets. An example is the data analyzed in [8], which was recorded under much lower stimulus onset asynchrony (175 ms instead of 1000 ms in the oddball data). ICA-based artifact reduction of this BCI data increased the classification error slightly, but significantly. This result may be explained by the fact, that target and non-target responses have lower amplitudes and are not separated as clearly as in the oddball data. Thus any class-discriminative activity may be contained in small-variance signal components which are harder to separate from artifactual components using ICA.

The fact that pre-filtering strongly influences the unmixing quality of ICA is highlighted by its strong impact on the percentage of near-dipolar ICA components. Consistent with the results obtained from the SNR, the dipolarity measure indicates that pre-filtering at very small frequencies < 0.5 Hz may not be optimal. In our analysis, high-pass filtering between 1 and 2 Hz consistently produced good results in terms of SNR, classification accuracy, and 'dipolarity' of the ICA decomposition. If information is contained in slow signal components, ICA can be trained on filtered data, and the learned weights can be applied to the unfiltered data.

ACKNOWLEDGMENT

We thank the authors of [12] for providing data and Stefan Haufe and Guido Nolte for advise on and implementation of MUSIC, respectively.

REFERENCES

[1] L. Frølich, T. S. Andersen, and M. Mørup, "Classification of independent components of EEG into multiple artifact classes," *Psychophysiology*, vol. 52, no. 1, pp. 32–45, 2015.
[2] A. Hyvärinen, J. Karhunen, and E. Oja, *Independent Component Analysis*. New York: John Wiley & Sons, 2001.
[3] D. M. Groppe, S. Makeig, and M. Kutas, "Identifying reliable independent components via split-half comparisons," *NeuroImage*, vol. 45, no. 4, pp. 1199 – 1211, 2009.
[4] Z. Zakeri, S. Assecondi, A. Bagshaw, and T. Arvanitis, "Influence of signal preprocessing on ICA-based EEG decomposition," in *XIII MEDICON 2013*, pp. 734–737.
[5] R. Scheeringa, P. Fries, K.-M. Petersson, R. Oostenveld, I. Grothe, D. G. Norris, P. Hagoort, and M. C. Bastiaansen, "Neuronal dynamics underlying high- and low-frequency EEG oscillations contribute independently to the human BOLD signal," *Neuron*, vol. 69, no. 3, pp. 572 – 583, 2011.
[6] A. Delorme, J. Palmer, J. Onton, R. Oostenveld, and S. Makeig, "Independent EEG sources are dipolar," *PLoS ONE*, vol. 7, no. 2, p. e30135, 02 2012.
[7] I. Winkler, S. Haufe, and M. Tangermann, "Automatic classification of artifactual ICA-components for artifact removal in EEG signals," *Behavioral and Brain Functions*, vol. 7, p. 30, 2011.
[8] I. Winkler, S. Brandl, F. Horn, E. Waldburger, C. Allefeld, and M. Tangermann, "Robust artifactual independent component classification for BCI practitioners," *J. Neural. Eng.*, vol. 11, no. 3, p. 035013, 2014.
[9] F. Ghaderi, S. K. Kim, and E. A. Kirchner, "Effects of eye artifact removal methods on single trial P300 detection, a comparative study," *Journal of Neuroscience Methods*, vol. 221, pp. 41 – 47, 2014.
[10] R. J. Croft and R. J. Barry, "Removal of ocular artifact from the EEG: a review," *Clinical Neurophysiology*, vol. 30, pp. 5–19, 2000.
[11] J. M. Pignat, O. Koval, D. V. D. Ville, S. Voloshynovskiy, C. Michel, and T. Pun, "The impact of denoising on independent component analysis of functional magnetic resonance imaging data," *Journal of Neuroscience Methods*, vol. 213, no. 1, pp. 105 – 122, 2013.
[12] M. Schreuder, T. Rost, and M. Tangermann, "Listen, you are writing! Speeding up online spelling with a dynamic auditory BCI," *Frontiers in Neuroprosthetics*, vol. 5, no. 112, 2011.
[13] S. Lemm, G. Curio, Y. Hlushchuk, and K.-R. Müller, "Enhancing the signal-to-noise ratio of ICA-based extracted ERPs," *Biomedical Engineering, IEEE Transactions on*, vol. 53, no. 4, pp. 601–607, 2006.
[14] B. Blankertz, S. Lemm, M. S. Treder, S. Haufe, and K.-R. Müller, "Single-trial analysis and classification of ERP components – a tutorial," *NeuroImage*, vol. 56, no. 2, pp. 814–825, 2011.
[15] R. Schmidt, "Multiple emitter location and signal parameter estimation," *Antennas and Propagation, IEEE Transactions on*, vol. 34, no. 3, pp. 276–280, 1986.
[16] A. Hyvärinen and E. Oja, "A fixed-point algorithm for independent component analysis," *Neural Computation*, vol. 7, pp. 1483–1492, 1997.
[17] S. Debener, J. Thorne, T. R. Schneider, and F. C. Viola, "Using ICA for the analysis of multi-channel EEG data," in *Simultaneous EEG and fMRI: Recording, Analysis, and Application*, M. Ullsperger and S. Debener, Eds. Oxford University Press, 2010.
[18] A. Widmann, E. Schröger, and B. Maess, "Digital filter design for electrophysiological data - a practical approach," *Journal of Neuroscience Methods*, 2014, in press.
[19] L. Bougrain, C. Saavedra, and R. Ranta, "Finally, what is the best filter for P300 detection?" in *TOBI Workshop lll-Tools for Brain-Computer Interaction*, 2014, pp. 734–737.
[20] J. Farquhar and N. Hill, "Interactions between pre-processing and classification methods for event-related-potential classification," *Neuroinformatics*, vol. 11, no. 2, pp. 175–192, 2013.
[21] S. Romero, M. Mañanas, and M. Barbanoj, "Ocular reduction in EEG signals based on adaptive filtering, regression and blind source separation," *Annals of Biomedical Engineering*, vol. 37, no. 1, pp. 176–191, 2009.